

Direct frequency comb generation from an octave-spanning, prismless Ti:sapphire laser

L. Matos and D. Kleppner

Department of Physics and Research Laboratory of Electronics, Massachusetts Institute of Technology, Cambridge, Massachusetts 02139

O. Kuzucu, T. R. Schibli, J. Kim, E. P. Ippen, and F. X. Kaertner

Department of Electrical Engineering and Computer Science and Research Laboratory of Electronics, Massachusetts Institute of Technology, Cambridge, Massachusetts 02139

Received December 5, 2003

We describe a self-referenced optical frequency comb generator based on an octave-spanning, prismless Ti:sapphire laser. Dispersion compensation is provided by novel double-chirped mirror pairs and BaF₂ wedges. Current versions operate at 80 and 150 MHz. The compact prismless design allows system scaling to a gigahertz repetition rate. Its carrier-envelope beat note is intrinsically stable with a signal-to-noise ratio of 30 dB in a 100-kHz bandwidth. The octave is reached at 25 dB below the average power level. The in-loop accumulated phase error is 1.4 rad (20 mHz to 1 MHz). The technique has the advantages of simplicity and stability compared with previous designs. © 2004 Optical Society of America

OCIS codes: 120.3940, 320.7090, 320.7160.

The use of femtosecond lasers for frequency comb generation has revolutionized the technology of frequency metrology in the past 5 years.^{1–3} A typical setup employs a Ti:sapphire laser that produces pulses in the 10–30-fs range. To broaden the laser spectrum to an octave to stabilize the comb by self-referencing, a photonic crystal fiber is often used.⁴ In this method the long-wavelength part of the spectrum is doubled and brought into interference with the short-wavelength part, permitting direct carrier-envelope offset frequency detection and stabilization.² However, coupling of the laser beam into the small core diameter of a high-index-contrast fiber limits the long-term stability of the system. This problem is of particular concern for the development of optical clocks (for which long-term signal averaging is necessary). It is therefore highly desirable to generate an octave-spanning spectrum directly from a compact and stable high-repetition-rate laser.

In this Letter we present octave-spanning spectra generated by prismless Ti:sapphire lasers operating at repetition rates of 80 and 150 MHz. An advantage of the prismless geometry is that it may allow scaling to gigahertz repetition rates. In this laser the required broadband dispersion compensation is provided by novel double-chirped mirror (DCM) pairs^{5,6} in combination with thin BaF₂ wedge pairs. The output frequency comb of the 80-MHz laser is f_{ceo} stabilized directly by the f -to- $2f$ method. This constitutes a major improvement over previous approaches, which include an octave-spanning Ti:sapphire laser that used a combination of chirped mirrors and a prism pair to produce a continuum directly in the oscillator^{7–9} and other high-repetition-rate sources¹⁰ that do not reach a high enough spectral power density over one octave and must therefore use the $2f$ -to- $3f$ scheme for carrier-envelope stabilization. To produce a full octave with a Ti:sapphire laser, precise dispersion compensation over a wide bandwidth is crucial. Lasers that rely

on prisms to provide the required dispersion compensation are highly sensitive to cavity alignment. The present prismless design is far less sensitive, and, as a result, the long-term mode-locking stability is greatly improved.

The lasers demonstrated here consist of astigmatically compensated x-folded cavities [see Fig. 1(a)].

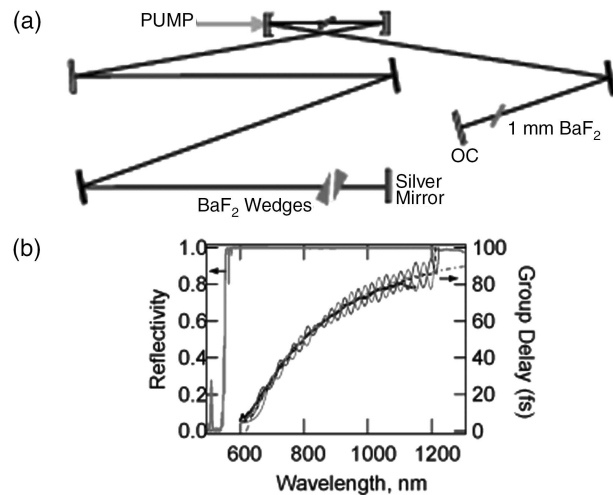


Fig. 1. (a) Schematic diagram of an octave-spanning prismless laser. Gray and black mirrors are type I and II DCMs, respectively. The BaF₂ wedges are used for fine tuning the dispersion. (b) Reflectivity of the type I DCMs with the pump window shown as a thick solid curve. The group-delay design is given by the thick dashed-dotted curve. The individual group delays of type I and II DCMs are shown as thin curves and their averages as a dashed curve, which is almost identical to the design goal over the wavelength range of interest from 650 to 1200 nm. The measured group delay, by use of white-light interferometry, is shown as the thick solid curve from 600 to 1100 nm. Beyond 1100 nm, the sensitivity of the Si detector limited the measurement.

They have a 2-mm-long Ti:sapphire crystal with an absorption of $\alpha = 7 \text{ cm}^{-1}$ at 532 nm. They are pumped by a diode-pumped, frequency-doubled Nd:vanadate laser. The radius of curvature of the folding mirrors is 10 cm, and the pump lens has a 60-mm focal length. All mirrors in the cavity, with the exception of the end mirrors, are type I (gray) and type II (black) DCMs that generate smooth group-delay dispersion when used in pairs.⁶ Figure 1(b) shows the reflectivity and group delay of the DCM pairs. The total group delay is smooth from 600 to 1200 nm. The average reflectivity over the full octave can be as high as 99.9%. One cavity end mirror is a silver mirror and the other is a broadband output coupler (OC) of either ZnSe/MgF₂ (80-MHz repetition-rate laser) or TiO₂/SiO₂ (150-MHz repetition-rate laser) coatings with 1% transmission. The output power in cw operation is typically 40 mW with 4.4 W of pump power. In mode-locked operation the average power is 90 mW.

In one round trip of the laser pulse through the cavity the 12 bounces on DCMs generate the precise negative dispersion required to compensate for the positive second- and third-order dispersion caused by the laser crystal, the air path in the cavity, and the BaF₂ wedge pairs used to fine tune the dispersion. We used BaF₂ for dispersion compensation because it has the lowest ratio of third- to second-order dispersion in the wavelength range from 600 to 1200 nm and the slope of the dispersion of BaF₂ is nearly identical to that of air. This makes it possible to scale the cavity length and repetition rate without changing the overall intracavity dispersion. To achieve mode-locked operation, it is necessary to reduce the amount of BaF₂ inside the laser cavity (i.e., by withdrawing one of the wedges). To achieve the broadest spectrum, the insertion of the BaF₂ wedge can be optimized. The spectral width of the laser is critically dependent on the dispersion balance, but, with prismless lasers, adjusting the dispersion does not significantly change the cavity alignment. In contrast with prism-compensated cavities, a slight misalignment of the resonator does not affect intracavity dispersion; therefore it is possible to operate the laser in an octave-spanning mode for as much as a full day without interruption. Figure 2(a) shows the spectrum under broadband operation of the 80-MHz laser. The octave is reached at a spectral density of ~ 25 dB below the average power level. The same plot shows the OC transmission curve. The detailed shape of this transmission curve is also a determining factor in the width of the output spectrum, since it significantly enhances the spectral wings.

Because the dispersion of 0.5 mm of BaF₂ is similar to that of 1 m of air, the cavity can be scaled up to gigahertz repetition rates by removing the air path and correspondingly adding BaF₂ to maintain the proper dispersion balancing. (This is not possible in lasers with intracavity prisms because a minimum distance between the prisms is required to provide negative dispersion.) Higher repetition rates are desirable for metrology not only because of their stability and compactness but also because they provide

increased power per mode in the comb for the same average output power.² As a first step in this direction, we constructed a 150-MHz repetition-rate laser that yields comparable spectra, as shown in Fig. 2(b).

To employ these broadband lasers as frequency comb generators, it is necessary to control the carrier-envelope offset frequency f_{ceo} and repetition rate f_{rep} . We directly measure f_{ceo} by the f -to- $2f$ technique described in Ref. 2. A dichroic beam splitter is used to split the laser output into long- and short-wavelength components and recombine them after insertion of a proper time delay stage [Fig. 3(a)]. The delay stage is essential to compensate for the difference in group delay between the 580- and 1160-nm radiation in the optical components. The recombined beam is then focused into a 1-mm BBO crystal cut for type I second-harmonic generation of 1160 nm. The resulting output is sent through a 10-nm-wide spectral filter centered at 580 nm. After projecting the doubled 1160-nm light and the fundamental into the same polarization to allow interference, the beat signal is detected by a photomultiplier tube (PMT). Figure 3(b) shows the detected f_{ceo} beat signal with 10- and 100-kHz measurement bandwidths. The signal-to-noise ratios are 30 and 40 dB, respectively. This signal is limited by the amount of power in the fundamental at 580 nm. An improved OC design, providing higher output coupling and therefore enhancing the short-wavelength part of the spectrum, should improve the signal-to-noise ratio. The f_{ceo} beat is intrinsically stable. In the absence of active feedback and without any temperature control of the breadboard the frequency stays within an 8-MHz window for more than 10 h. On the time scale of seconds, it can jitter by ~ 100 kHz.

To implement the lock we filter component $f_{\text{rep}} + f_{\text{ceo}}$ at 130 MHz from the PMT signal and phase lock it to a rf synthesizer using a phase-locked loop. To increase the locking range, the 130-MHz signal is properly filtered, amplified, sent to a 32-fold frequency divider, and then compared with the synthesizer signal in a digital phase detector. The phase error signal controls the pump power via an acousto-optic modulator, which directly controls the carrier-envelope frequency of the laser.³ In lasers with intracavity prisms the transducer that controls f_{ceo} is often a piezo-driven

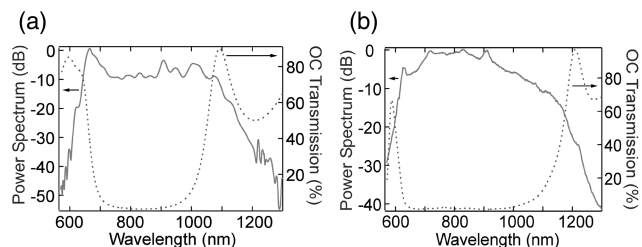


Fig. 2. Measured output spectrum for lasers with (a) 80-MHz repetition rate and (b) 150-MHz repetition rate. In both cases the octave is reached at ~ 25 dB below the average power level. The average mode-locked power is 90 mW for both lasers. Also shown (dotted curves) are the respective OC transmission curves for (a) the ZnSe/MgF₂ Bragg stack and (b) a broadband SiO₂/TiO₂ stack. Both have $\sim 1\%$ transmission at 800 nm.

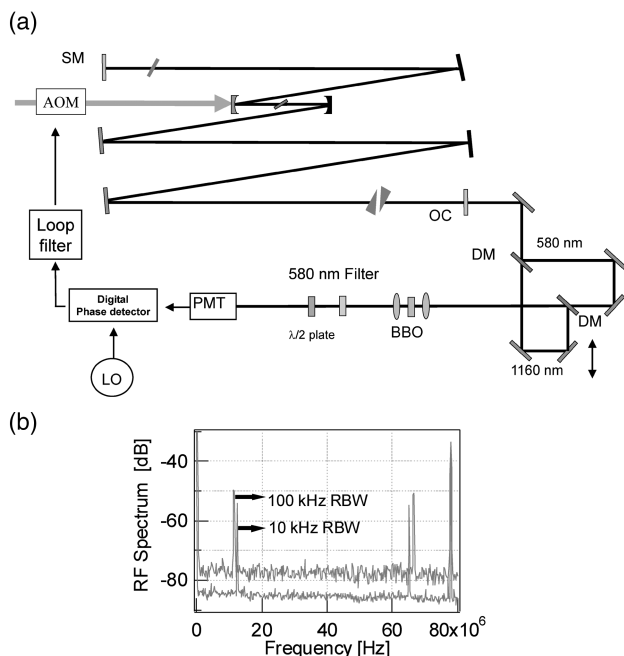


Fig. 3. (a) Setup for f_{ceo} detection and lock (see text). SM, silver mirror; DM, dichroic mirror; LO, local oscillator. (b) Measured carrier-envelope beat signal from the 80-MHz laser with 10- and 100-kHz resolution bandwidths (RBW).

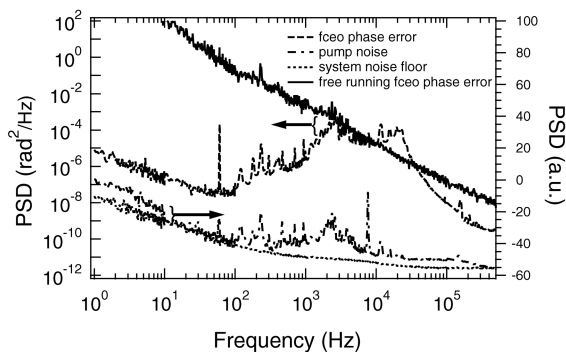


Fig. 4. Spectral densities of the phase error signal at the output of the digital phase detector for the f_{ceo} lock (dashed curve) and free-running f_{ceo} (solid curve), with the scale on the left. Spectral density of the pump noise recorded in the absence of f_{ceo} feedback (dashed-dotted curve) and system noise floor (dotted curve), with the scale on the right. The major contribution to f_{ceo} noise is due to pump noise. PSD, phase error spectral density.

tilting end mirror.¹¹ In a prismless cavity we can use modulation of the pump power to control f_{ceo} .

Figure 4 shows the measured phase error spectral densities of the f_{ceo} beat with and without active stabilization. The integrated phase error for the in-loop measurement is 1.4 rad (from 50 mHz to 1 MHz). The major contribution to this phase noise error comes from

the pump noise shown in relative units in Fig. 4. The spectral components from 1–10 kHz contribute 90% of the phase error. However, this comb can be used for metrology because no cycle slips occur. An improved loop filter design for stronger noise suppression and a pump laser with lower noise to achieve lower residual carrier-envelope phase fluctuations are being implemented.

In summary, we have demonstrated a stabilized frequency comb from an octave-spanning prismless Ti:sapphire laser that can be scaled to high repetition rates of several hundred megahertz and possibly gigahertz. Repetition-rate scaling is allowed by the use of BaF₂ material for dispersion compensation, which can be used to compensate for the reduced amount of air inside the high-repetition-rate resonator over almost one octave of bandwidth. Such a compact and long-term stable frequency comb generator may serve as the clockwork for future optical clocks as well as a source of phase-controlled optical pulses for phase-sensitive nonlinear optical experiments.

The authors gratefully acknowledge fruitful discussions with Jun Ye and David Jones. This work was supported in part by MIT Lincoln Laboratory grant ACC-334, National Science Foundation grant ECS-0119452, U.S. Air Force Office of Scientific Research grant F49620-01-1-0084, and Office of Naval Research grant N00014-02-1-0717. L. Matos's e-mail address is lia@mit.edu.

References

1. T. Udem, J. Reichert, R. Holzwarth, and T. Hänsch, *Phys. Rev. Lett.* **82**, 3568 (1999).
2. D. J. Jones, S. A. Diddams, J. K. Ranka, A. Stentz, R. S. Windeler, J. L. Hall, and S. T. Cundiff, *Science* **288**, 635 (2000).
3. R. Holzwarth, T. Udem, T. W. Hänsch, J. C. Knight, W. J. Wadsworth, and P. St. J. Russell, *Phys. Rev. Lett.* **85**, 2264 (2000).
4. A. Bartels, T. Dekorsy, and H. Kurz, *Opt. Lett.* **24**, 996 (1999).
5. F. X. Kärtner, U. Morgner, T. R. Schibli, E. P. Ippen, J. G. Fujimoto, V. Scheuer, G. Angelow, and T. Tschudi, *J. Opt. Soc. Am. B* **18**, 882 (2001).
6. T. R. Schibli, O. Kuzucu, J. Kim, E. P. Ippen, J. G. Fujimoto, F. X. Kärtner, V. Scheuer, and G. Angelow, *IEEE Sel. Top. Quantum Electron.* **9**, 990 (2003).
7. U. Morgner, R. Ell, G. Metzler, T. R. Schibli, F. X. Kärtner, J. G. Fujimoto, H. A. Haus, and E. P. Ippen, *Phys. Rev. Lett.* **86**, 5462 (2001).
8. R. Ell, U. Morgner, F. X. Kärtner, J. G. Fujimoto, E. P. Ippen, V. Scheuer, G. Angelow, and T. Tschudi, *Opt. Lett.* **26**, 373 (2001).
9. T. M. Fortier, D. J. Jones, and S. T. Cundiff, *Opt. Lett.* **28**, 2198 (2003).
10. A. Bartels and H. Kurz, *Opt. Lett.* **27**, 1839 (2002).
11. S. T. Cundiff, J. Ye, and J. L. Hall, *Rev. Sci. Instrum.* **72**, 3749 (2001).